International Immunopharmacology 67 (2019) 268–280

Contents lists available at ScienceDirect

International Immunopharmacology

journal homepage: www.elsevier.com/locate/intimp

Exosomes derived from mesenchymal stem cells attenuate inflammation and demyelination of the central nervous system in EAE rats by regulating the polarization of microglia

Zijian Li[a], Fei Liu[a], Xin He[a], Xue Yang[a], Fengping Shan[b], Juan Feng[a,*]

[a] Department of Neurology, Shengjing Hospital of China Medical University, No. 36 Sanhao Street, Heping District, Shenyang, Liaoning 110004, China
[b] Department of Immunology, School of Basic Medical Science, China Medical University, No. 77, Puhe Road, Shenyang, Liaoning 110122, China

ARTICLE INFO

Keywords:
Mesenchymal stem cells
Exosomes
Experimental autoimmune encephalomyelitis
Microglia
Polarization
Immunoregulation

ABSTRACT

Multiple sclerosis (MS) is a chronic demyelinating disease caused by central nervous system (CNS) inflammation and immune dysfunction, which often leaves patients with severe physical disabilities. Microglia function in the surveillance of the CNS, and an imbalance in the M1/M2 phenotypes of microglia contribute to the progression of MS. Recent studies indicate that exosomes secreted by bone marrow mesenchymal stem cells (BMSCs) play therapeutic roles in many autoimmune diseases and aid in tissue repair. However, it is not clear whether BMSC-derived exosomes can attenuate MS-associated inflammation and immune dysfunction, or how BMSC exosomes protect neurons. The experimental autoimmune encephalomyelitis (EAE) rat model was used to investigate the effect of exosomes on microglia polarization and inflammation in CNS. The results showed that exosome treatment significantly decreased neural behavioral scores, reduced the infiltration of inflammatory cells into the CNS, and decreased demyelination in comparison to untreated EAE rats. In addition, exosome treatment resulted in significant increases in the levels of M2-related cytokines such as interleukin (IL)-10 and transforming growth factor (TGF)-β, whereas M1-related tumor necrosis factor (TNF)-α and IL-12 levels decreased significantly. Moreover, compared with the untreated EAE group, the exosome group displayed significantly increased protein and mRNA expression levels of M2 phenotype markers, whereas M1 marker expression decreased. Our findings were further confirmed in an in vitro HAPI microglia cell line model. In conclusion, these findings indicate that BMSC-derived exosomes can attenuate inflammation and demyelination of the CNS in the EAE rat model by regulating the polarization of microglia. Therefore, the use of BMSC-derived exosomes may be a potential therapeutic approach for the treatment of autoimmune and inflammatory diseases.

1. Introduction

Multiple sclerosis (MS) is a severe autoimmune demyelinating disease of the central nervous system (CNS) that often leaves young adults permanently disabled and decreases their quality of life [1]. > 2.5 million people suffer from MS worldwide, resulting in a significant global health burden [2]. The experimental autoimmune encephalomyelitis (EAE) animal model is one of the most employed animal models in MS research, as both the clinical and pathological features of the model resemble those of MS patients [3]. Although significant progress has been made in the treatment of MS over the last decade, the current therapeutic strategies remain limited. Therefore, there is a critical need for new types of drugs or therapies.

As the resident macrophages of the CNS, microglia play vital roles in balancing the immune response, regulating inflammation, and promoting tissue repair [4]. In the initial stages of MS and EAE, inflammatory cells infiltrate the brain and spinal cord following damage to the blood-brain barrier (BBB). Microglia become abnormally activated, and this leads to demyelination and neurodegeneration [5]. The M1 microglia phenotype, which is the phenotype that causes tissue damage in the CNS through the release of pro-inflammatory cytokines, is predominant in the early stages of MS. However, microglia with an

Abbreviations: MS, multiple sclerosis; CNS, central nervous system; EAE, experimental autoimmune encephalomyelitis; IL, interleukin; TGF, transforming growth factor; TNF, tumor necrosis factor; BBB, blood-brain barrier; BMSC, bone marrow mesenchymal stem cells; PBS, phosphate buffered solution; PE, P-phycoerythrin; FITC, fluorescein isothiocyanate; OCT, optimum cutting temperature compound; TEM, transmission electron microscopy; HE, hematoxylin-eosin; LFB, Luxol Fast Blue; iNOS, inducible nitric oxide synthase; BSA, bovine serum albumin; ELISA, enzyme-linked immunosorbent assay; NO, nitric oxide; Arg1, arginase-1

* Corresponding author.
E-mail addresses: zjli@cmu.edu.cn (Z. Li), juanfeng@cmu.edu.cn (J. Feng).

https://doi.org/10.1016/j.intimp.2018.12.001
Received 3 September 2018; Received in revised form 12 November 2018; Accepted 1 December 2018
Available online 17 December 2018

M2 phenotype can produce anti-inflammatory cytokines and promote tissue regeneration [6]. Therefore, it is believed that an M1/M2 phenotype imbalance participates in the occurrence and development of MS, and that the polarization of microglia from the M1 to the M2 phenotype can restore immune homeostasis and improve neurological function in those with MS [7].

Mesenchymal stem cells (MSCs) are a type of multipotent cell with great potential in the field of biotherapy, particularly in the areas of immunoregulation and tissue regeneration [8–10]. Exosomes, with a diameter of 30–120 nm, are small cell-derived, membrane-enclosed vesicles that may contain proteins, lipids, and microRNAs from their parent cells [11,12]. In recent years, increasing evidence has strongly suggested that exosomes play a key role during stem cell therapy, acting through a paracrine mechanism [13,14]. Exosomes have attracted significant attention from clinicians and researchers due to their stability in circulation and low immunogenicity compared to that of stem cells [15,16]. Previous studies have demonstrated that exosomes derived from bone marrow MSCs (BMSC exosomes) can exert an immunoregulatory effect in different autoimmune related disorders [17,18], attenuate tissue injury and promote tissue repair [19–23]. Therefore, we hypothesized that BMSC exosomes could provide a better course of treatment for EAE. Thus, the purpose of this study was to determine whether intravenously administered BMSC exosomes could restore neurological function in EAE rats. Furthermore, we investigated whether treatment with BMSC exosomes would impact microglia polarization in vivo and in vitro. Further studies in this field will improve the understanding of the precise mechanism of autoimmune diseases and may lead to novel therapeutics and preventative strategies.

2. Materials and methods

2.1. Animals

Male Sprague Dawley (SD) rats (80–100 g), female SD rats (200–220 g), and guinea pigs (350–450 g) were provided by the Research and Development Center of Shengjing Hospital (Shenyang, China). Animals were housed with free access to food and water under a natural day/night cycle. The experiments were performed in adherence to the guidelines for the Care and Use of Laboratory Animals of the National Institutes of Health. All efforts were made to minimize the number of animals used and their suffering. This study was approved by the Institutional Animal Care and Use Committee of Shengjing Hospital, China Medical University (No. 2016PS012K).

2.2. Reagents

CellTiter 96® AQueous One Solution Cell Proliferation Assay was purchased from Promega (Madison, WI, USA), which was performed for MTS detection. Flow cytometry antibodies, including anti-CD29-PE, anti-CD44-FITC, anti-CD45-FITC and anti-CD90-PE were purchased from Biolegend (San Diego, CA, USA). Anti-CD34-PE antibody was purchased from Abcam (Cambridge, MA, USA). Anti-CD73-FITC antibody was purchased from Bioss (Boston, MA, USA). CD105 primary antibody and Goat anti-rabbit IgG-FITC second antibody were purchased from Absin (Shanghai, China). SD rat bone marrow mesenchymal stem cell osteogenic, adipogenic and chondrogenic differentiation basal medium were purchased from Cyagen Biosciences (Guangzhou, China). Anti-CD9 and anti-CD63 antibodies for western blotting were purchased from Abcam (Cambridge, MA, USA), and anti-Alix antibody was purchased from Cell Signaling Technology (Beverly, MA, USA). Agents used for EAE induction include Pertussis Toxin (Millipore, USA), incomplete Freund's adjuvant (Sigma, St. Louis, MO, USA), and *Mycobacterium tuberculosis* H37Ra (Difco; BD Biosciences, USA). Optimum cutting temperature compound (OCT) was purchased from Thermo Fisher (Waltham, MA, USA). Hematoxylin-Eosin (HE) stain and Luxol Fast Blue (LFB) stain regents were purchased from Beyotime (Shanghai, China) and Sigma (St. Louis, MO, USA), respectively. Immunofluorescence primary antibodies, including anti-CD68 and anti-CD206, were purchased from Abcam (Cambridge, MA, USA). Reverse transcription of total RNA and real-time qPCR were performed using PrimeScript™ RT Master Mix and SYBR® Premix Ex Taq™, respectively, which were purchased from Takara (Nojihigashi, Shiga, Japan). ELISA kits for rat tumor necrosis factor alpha (TNF-α), transforming growth factor beta (TGF-β), interleukin-10 (IL-10), and IL-12 were purchased from Dakewe Biotech Co., Ltd. (Shenzhen, China).

2.3. Isolation and culture of primary bone marrow MSCs

Primary bone marrow MSCs were isolated from all anesthetized (under 1% sodium pentobarbital, 40 mg/kg intraperitoneal injection) male rats (80–100 g) as previously described [24]. Briefly, bone marrow cells from the femur were flushed with culture medium and seeded in culture dishes containing Dulbecco's modified Eagle's medium (DMEM)-low glucose (Biological Industries) supplemented with 10% fetal bovine serum (Biological Industries) and 1% penicillin/streptomycin (Biological Industries). Cells were then incubated at 37 °C in a humidified atmosphere containing 5% CO_2. After 48 h, the media was changed to remove the nonadherent cells. Once the cells had grown to 80% confluence, they were harvested with 0.25% trypsin (Biological Industries) and passaged at a ratio of 1:3. Bone marrow MSCs were used for experiments at passages 3 (P3)–P5. The cell morphology was visualized and captured by a microscope (Nikon 300). MTS assay was performed to measure the expansion potential of P3, P4 and P5 MSCs. Briefly, bone marrow MSCs were seeded onto eight 96-well plates at 5000 cells/well under 37 °C, 5% CO_2 for 24 h. From the second day to the ninth day, one of the eight plates was selected randomly each day. Pipet 20 μL of CellTiter 96® AQueous One Solution Reagent (3-(4,5-dimethylthiazol-2-yl)-5-(3-carboxymethoxyphenyl)-2-(4-sulfophenyl)-2H-tetrazolium, inner salt; MTS) (Promega, Madison, WI, USA) into each well of the 96-well assay plate containing the samples in 100 μL of culture medium. Incubate the plate at 37 °C for 3 h in a humidified, 5% CO_2 atmosphere. Record the absorbance at 490 nm using a multi-detection microplate reader (BioTek, USA). Background absorbance of only medium was subtracted. Each assay was carried out in triplicate. According the results of MTS assay every day, draw the growth curve and detect the cell expansion potential.

2.4. Flow cytometry

MSCs were cultured in T75 cell culture flasks (Nest, China). The cells were then collected and tested. The MSCs at P3 were suspended in phosphate buffered saline solution (PBS) with 1% BSA, then incubated and distributed into tubes at a concentration of 1×10^7 cells/mL (100 μL/tube). The cells were then incubated with antibodies (CD29-PE, CD34-PE, CD44-FITC, CD45-FITC, CD73-FITC, CD90-PE and CD105-FITC) on ice for 15 min in the dark. MSCs were washed 2 times with at least 2 mL of PBS with 1% BSA and centrifuged at 800 rpm for 5 min. These cells were analyzed with a BD FACSCalibur flow cytometer (BD Biosciences). CellQuest for Mac v3.0 (BD Biosciences) was used to analyze the phenotypes of the cells.

2.5. Osteogenic, adipogenic and chondrogenic differentiation of MSCs

To identify the differentiation properties of primary BMSCs, P3 BMSCs were seeded in a 6-well plate (2×10^4 cells/cm^2) and cultured in multipotent differentiation induction medium. The 6-well plates used for osteogenic differentiation were coated with 0.1% gelatin solution in advance. When the cell density reached 60–70%, the complete medium was replaced with osteogenic differentiation induction medium. The medium was exchanged for fresh induction media every 3 days for about 4 weeks at all. For adipogenic differentiation, cell density was allowed to reach 100% before the media was exchanged for adipogenic

differentiation induction media. Use of adipogenic differentiation induction media A and B was alternated, and the cells were cultured in this media for about 4 weeks. For chondrogenic differentiation, P3 MSCs were trysinized and counted after fusion growth. 4×10^5 cells were transfer to a 15 mL centrifuge tube and centrifuged 4 min at the speed of 250 ×*g*. Remove the supernatant. Wash the cells with culture medium for 2 times, centrifuged 5 min at the speed of 150 ×*g*. Use the centrifuge tube as the chondrogenic differentiation container. When cells gathered after the first seeded, flick pipe bottom for suspension cultivation. The medium was exchanged for fresh induction media every 2–3 days for about 4 weeks at all. The differentiated cells were fixed and stained with Alizarin Red Solution, Oil Red O Solution and Alcian Blue Solution to analyze osteogenesis, adipogenesis and chondrogenesis, respectively.

2.6. Isolation and identification of BMSC-derived exosomes

Exosomes were isolated from the cell culture media of BMSCs by ultra-centrifugation as previously described [25]. Briefly, BMSCs were cultured for 48 h in media with exosome free serum, and the culture medium was collected and centrifuged at 300 ×*g* for 10 min, 2000 ×*g* for 10 min, 10,000 ×*g* for 30 min, and 100,000 ×*g* for 70 min twice using an ultracentrifuge (CS120FNX, HITACHI, Japan). Anti-Alix (1:1200), anti-CD63 (1:1000), and anti-CD9 (1:2000) antibodies were used to evaluate the characteristics of the isolated exosomes by western blot. The enriched exosomes were also analyzed using transmission electron microscopy (TEM) as previously described. First, the enriched exosomes were loaded onto a copper wire mesh and allowed to sit for 5 min to enable precipitation. The copper wire mesh was then placed at room temperature for 30 min to remove the excess fluid. The samples were then stained in 10 μL of neutral 1% phosphotungstic acid for negative staining. Samples were naturally air dried at room temperature and observed by TEM at 80 kV. 10 fields of view in each sample were randomly chosen and photographed at 70,000×.

2.7. EAE induction and neurobehavioral analysis

EAE models were established as previously described [26]. Firstly, guinea pigs (350–450 g) were anesthetized (under 1% sodium pentobarbital, 40 mg/kg intraperitoneal injection) to obtain guinea pig spinal cord (on the ice plate) which was the main antigenic component of molding agents. Then the female rats (200–220 g) were anesthetized with 1% pentobarbital, and each rat was immunized subcutaneously with a 400 μL emulsion mixture composed of guinea pig spinal cord homogenate (1 g guinea pig spinal cord in 1 mL 0.9% saline) and an equal volume of incomplete Freund's adjuvant (Sigma, St. Louis, MO, USA) containing 10 mg/mL *Mycobacterium tuberculosis* H37Ra (Difco; BD Biosciences, USA) in both hind footpads and in the base of the tail. The day of immunization is designated as day 0 (D0). Adult female rats were randomly divided into five groups (n = 8 per group): (1) control group; (2) EAE group; (3) exosomes-low dose group (EAE + exosomes 100 μg); (4) exosomes-high dose group (EAE + exosomes 400 μg); (5) BMSCs group (EAE + BMSCs = 10^6 in equal volume of vehicle PBS). Tail vein injection of MSC-derived exosomes or BMSCs was performed 24 h after EAE induction. The control group rats were injected with an amount of vehicle equal to that given to the experimental groups. The doses used in these experiments are consistent with those used in similar previous studies [19,23,27,28]. During the course of the experiment, body weights and neurobehavioral scores of the rats were monitored once daily by two independent observers in a blinded fashion. Neurobehavioral scores were defined by the following scale: 0 = without any clinical symptoms; 1 = reeling gait or loss of tail tension; 2 = flaccid tail, hindlimb weakness; 3 = hindlimb paralysis; 4 = hindlimb paralysis, forelimb paralysis, or forelimb weakness with urinary and defecation dysfunction; 5 = moribund or dead; the sign between two of them ± 0.5. In our preliminary experiments, the disease peak period was between days 12 and 14 post-immunization. All the rats were sacrificed at day 15 and the spinal cord tissue in the vertebral lumbar enlargement and brain tissue were collected.

2.8. Histological examination

Sacrificed rats were transcardially perfused with normal saline and 4% paraformaldehyde. The brain and the lumbar enlargements of the spinal cord were fixed in 4% paraformaldehyde for 24 h, embedded in paraffin, and cut into sections of 4–5 μm thickness. To evaluate the extent of inflammatory cell infiltration, hematoxylin-eosin (HE) staining was performed according to the manufacturer's instructions. Meanwhile, to evaluate the extent of demyelination, Luxol Fast Blue (LFB) staining was performed as previously reported [29]. Briefly, spinal cord sections were incubated in 0.1% LFB solution at 60 °C overnight and then differentiated in 0.05% lithium carbonate and 70% ethanol. The images were observed and captured using a Nikon 300 microscope equipped with a digital camera. In our experiments, 3 histological sections were analyzed per rat, and their average scores were calculated. The extent of demyelination was scored according to the following criteria: none = 0; rare foci = 1; a few areas of demyelination = 2; large or confluent areas of demyelination = 3. Inflammatory infiltration was scored as follows: no infiltrating cells = 0; a few scattered infiltrating cells = 1; organization of inflammatory infiltration around blood vessels = 2; extensive perivascular cuffing with widespread infiltration = 3 [30].

2.9. Immunofluorescent staining

Frozen brain and spinal cord tissue sections were obtained as previously descried [31]. Briefly, the brain and spinal cord tissue of the sacrificed rats was extracted and fixed in 4% paraformaldehyde overnight. The tissues were then dehydrated with 15% and 30% sucrose solutions successively, embedded in optimum cutting temperature compound (OCT), and cut into 15 μm thick sections with a cryostat microtome (Leica, Germany). The frozen sections and 4% paraformaldehyde fixed cell culture-treated coverslips were washed with PBS and blocked in 5% BSA for 30 min at room temperature. They were then incubated at 4 °C overnight with the primary antibodies, including anti-CD68 (1:100) and anti-CD206 (1:500). Then sections were washed with PBS and incubated with the corresponding secondary antibody (R-PE–conjugated donkey anti-mouse IgG (1:100) or Fluorescein (FITC)–-conjugated AffiniPure donkey anti-rabbit IgG (1:100)) for 3 h at room temperature. Nuclei were stained with 4,6-diamidino-2-phenylindole (DAPI, Sigma) for 5 min. Fluorescent images were visualized and captured by a fluorescence microscope (Nikon 300).

2.10. Cell line culture

In in vitro study, rat highly aggressive proliferating immortalized (HAPI) microglial cell line CRL-2815® (ATCC, USA) was cultured with DMEM-high glucose (Biological Industries) supplemented with 10% FBS and 1% penicillin/streptomycin. The cells were then incubated at 37 °C in a humidified atmosphere containing 5% CO_2. The medium was renewed for every 2–3 days.

2.11. ELISA

The levels of cytokines in cell culture supernatants and serum from rats were determined by enzyme-linked immunosorbent assay (ELISA). ELISA kits for rat tumor necrosis factor alpha (TNF-α), interleukin-12 (IL-12), transforming growth factor beta (TGF-β), and interleukin-10 (IL-10) were purchased from Dakewe Biotech Co., Ltd. and used according to the manufacturer's instructions. The experiments were all performed in triplicate. The concentrations were quantified with reference to the standard curve and detected by a multi-detection

Table 1
Sequences of primers used for qPCR.

Gene	Gene bank accession		Sequence
TNF-α	NM_012675	Forward	5′-CCACGCTCTTCTGTCTACTG-3′
		Reverse	5′-GCTACGGGCTTGTCACTC-3′
iNOS	NM_012611	Forward	5′-ATCCCGAAACGCTACACTT-3′
		Reverse	5′-CGGCTGGACTTCTCACTC-3′
IL-10	NM_012854	Forward	5′-CAGTCAGCCAGACCCACAT-3′
		Reverse	5′-GGCAACCCAAGTAACCCT-3′
TGF-β	NM_031131	Forward	5′-ATCCCGCCCACTTTCTAC-3′
		Reverse	5′-CCGTTGTTCAGCCACTCT-3′
Arg-1	NM_017134	Forward	5′-CAGTGGCGTTGACCTTGT-3′
		Reverse	5′-TGGTTCTGTTCGGTTTGC-3′
GAPDH	NM_017008	Forward	5′-GCAAGTTCAACGGCACAG-3′
		Reverse	5′-GCCAGTAGACTCCACGACAT-3′

microplate reader at 450 nm.

2.12. Real-time PCR analysis

To detect the mRNA levels of M1 and M2 microglia markers, total RNA was isolated from the brain (white matter around the lateral ventricle), spinal cord (lumber enlargement) tissue, and microglia using TRIzol reagent according to the manufacturer's instructions. Reverse transcription from total RNA to cDNA and quantitative real-time PCR were performed using the Takara PrimeScript RT Master Mix and SYBR Green Premix, respectively. The primers used in this study are listed in Table 1. The results were analyzed using the $2-\Delta\Delta Ct$ method and represented as fold changes, normalized to GAPDH.

2.13. Co-culture experiments

To determine whether cell-to-cell contact was required for BMSCs to exert their effects upon HAPI microglia cells or whether paracrine action was involved, the transwell co-culture system was utilized. It was made up of 12-well Millicell® Hanging Cell culture Insert (pore size = 0.4 μm, Millipore, USA) and its matched 12-well plate. BMSCs were seeded in the upper chamber and HAPI microglia cells were seeded in the lower chamber, and HAPI microglia cells were treated with or without LPS. Soluble factors could pass through the membrane of the chamber freely. Untreated microglia were used as a control. The microglia in the lower chamber were collected for RNA and protein extraction. The supernatants were then collected for nitric oxide (NO) detection and ELISA.

2.14. Nitrite detection

As NO usually exists in the form of nitrite in cells, we evaluated the production of NO by detecting the accumulation of nitrite in the cell culture supernatant using the one-step NO testing kit (JianCheng, Nanjing, China). First, LPS-activated HAPI microglia cells were incubated in a 6-well plate for 48 h, in which different concentrations with equal volume (62.5, 125, 250, 500, or 1000 μg/mL) of BMSC exosomes were added. LPS-activated HAPI microglia cells were used as positive control and untreated microglia were used as a negative control. In addition, the supernatants from the co-culture system were collected as a group. The regents from the NO testing kit were then mixed with the supernatants in a 96-well plate, and the assay was performed according to the manufacturer's instructions. The concentrations were calculated using a standard curve and measured by a multi-detection microplate reader at 550 nm.

2.15. Shotgun proteomic analysis

We mixed 3 replicate samples of exosomes derived from BMSCs into a pooled sample and sent it for shotgun proteomic analysis. Briefly, SDT buffer (4% SDS, 100 mM Tris-HCl, 1 mM DTT, pH 7.6) was added to the sample. The lysate was sonicated and then boiled for 10 min. After centrifuged at 13,400 × *g* for 30 min. Then the proteins were performed filter-aided sample preparation (FASP) digestion. The detergent, DTT and other low-molecular-weight components were removed using UA buffer (8 M urea, 150 mM Tris-HCl pH 8.0) by repeated ultrafiltration (Microcon units, 10 kD). Then 100 μL iodoacetamide (100 mM IAA in UA buffer) was added to block reduced cysteine residues and the samples were incubated for 30 min in darkness. The filters were washed with 100 μL UA buffer three times and then 100 μL 25 mM NH_4HCO_3 buffer twice. Finally, the protein suspensions were digested with 4 μg trypsin (Promega) in 40 μL 25 mM NH_4HCO_3 buffer overnight at 37 °C, and the resulting peptides were collected as a filtrate. The peptides of each sample were desalted on C18 Cartridges (Empore™ SPE Cartridges C18 (standard density), bed I.D. 7 mm, volume 3 mL, Sigma), concentrated by vacuum centrifugation and reconstituted in 40 μL of 0.1% (v/v) formic acid. The peptide content was estimated by UV light spectral density at 280 nm. LC-MS/MS analysis was performed on a Q Exactive mass spectrometer (Thermo Scientific) that was coupled to Easy nLC (Proxeon Biosystems, now Thermo Fisher Scientific) for 120 min.

2.16. Statistical analysis

Statistical analysis was performed using GraphPad Prism 5.0 (San Diego, CA, USA). Student's *t*-test and one-way ANOVA were used to evaluate the differences among groups. A P value < 0.05 was considered to be statistically significant. The data are expressed as mean ± standard deviation (SD). The in vitro experiments were performed at least three times to verify the reproducibility.

3. Results

3.1. Identification of BMSCs

Before primary BMSCs were used in experiments, we confirmed that they met the three minimal standards for defining MSCs [32]. First, MSCs should adhere to the bottom of a plastic flask in standard culture conditions. When cultured to P3, the BMSCs gradually began to display a fibroblast-like, spindle-shaped morphology and gather together in a circinate appearance (Fig. 1A), as observed by inverted phase contrast microscopy. The expansion potential of P3 to P5 MSCs was detected by MTS assay and the line chart was draw (Fig. 1A). Secondly, cultured BMSCs were CD29, CD44, CD73, CD90 and CD105 positive but negative for CD34 and CD45 (Fig. 1B). The purity of MSCs in culture was examined up to 95%. And no obvious morphological changes were observed within the P3 to P5. After culturing BMSCs in osteogenic differentiation induction media for 3 weeks, the cells were positively stained by the Alizarin Red solution. After 4 weeks of culture in adipogenesis induction media, oil droplets were observed in the cells. And after 4 weeks of culture in chondrogenesis induction media, acidic mucopolysaccharides were observed by Alcian Blue staining. Finally, we were able to successfully perform osteogenic, adipogenic and chondrogenic induction from P3 BMSCs (Fig. 1C).

3.2. Identification of BMSC exosomes

BMSCs were cultured in DMEM-LG medium with 10% exosome-free FBS for 48 h, which was made by ultracentrifuging the FBS at 100,000 × *g* for 21 h at 4 °C and filtering the resulting supernatant with a 0.22 μm filter (Millipore, Massachusetts, USA). Then, we purified exosomes from the culture supernatants of BMSCs using differential centrifugation methods. TEM results showed that the isolated exosomes had a bilayer membrane structure with a diameter of 30–100 nm (Fig. 1D). Furthermore, equal amounts of protein were extracted from BMSCs and BMSC exosomes for western blotting to confirm the

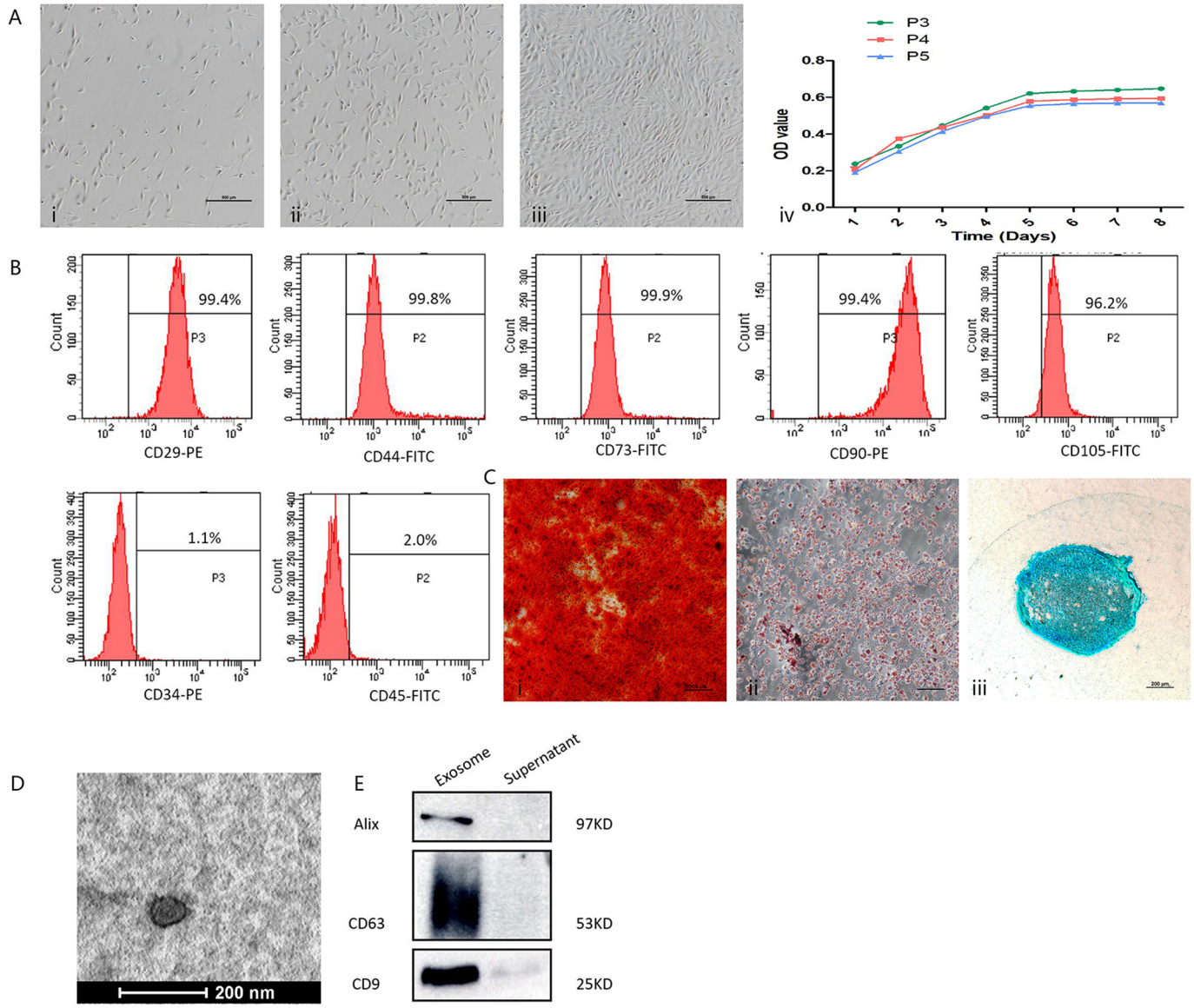

Fig. 1. Culture and identification of primary BMSCs and identification of BMSC exosomes. (A) Phase-contrast image of primary BMSC (i) P0 at day 1, (ii) P0 at day 3, and (iii) P1 at day 10 (scale bar = 500 μm), (iv) the line chart of MTS assay. (B) Flow cytometric phenotyping of BMSCs. (C) Multi-differentiation potential of BMSCs. (i) Alizarin Red staining of osteogenic mineralization (3 weeks). (ii) Oil Red O staining of small lipid droplets (4 weeks). (iii) Alcian Blue staining of acidic mucopolysaccharides (4 weeks) (scale bar = 200 μm). (D) Morphologic observation of BMSC-derived exosomes by transmission electron microscopy (scale bar = 200 nm). (E) Surface exosomal markers (Alix, CD63, and CD9) were analyzed by Western blotting BMSC exosomes and cell culture supernatants. (For interpretation of the references to color in this figure legend, the reader is referred to the web version of this article.)

expression of Alix, CD63, and CD9 (Fig. 1E), which are three widely recognized molecular markers for exosomes.

3.3. Effect of BMSC exosomes on clinical signs of EAE

To determine whether BMSC-derived exosomes alleviate clinical symptoms associated with EAE, rat neurobehavioral scores and body weight measurements were recorded after EAE induction and exosome treatment. Higher neurobehavioral scores and lower weights indicate the deterioration of motor dysfunction and increased disease severity. In our preliminary experiments, the rats began to get sick at about day 9–10, the illness peaked at day 14, and by day 21, the rats had recovered. In our present study, the rats in the EAE group were showing neurobehavioral signs and losing body weight by day 10 after immunization (Fig. 2A), which is similar to our previous studies [29]. The neurological scores rapidly increased in the EAE group in the following days and reached their peak at day 14. As illustrated in Fig. 2A, BMSC treatment significantly attenuates EAE severity in rats. To investigate whether BMSC exosomes could play a therapeutic role in vivo similar to BMSCs, EAE rats were randomly grouped and injected with low or high doses of BMSC exosomes via the tail vein immediately after establishment of EAE. The neurobehavioral scores of the two BMSC exosome-treated groups were also increased at Day 10 but increased at a lower rate compared to the EAE group. Clinical sign scores in the EAE group were significantly increased compared to the control group. Significant relief was observed in the exosome and BMSC-treated rats, which showed a significantly slower increase in clinical scores and reduced severity relative to the EAE group ($P < 0.05$; Fig. 2A). The body weights of the rats in the EAE group significantly decreased compared with those of rats in the control group ($P < 0.05$). Rats treated with exosomes and BMSCs showed dramatically higher weights compared to the EAE group at day 10 ($P < 0.05$). Significant differences were seen between the exosome-treated and BMSC-treated groups from day 10 to 14 ($P < 0.05$; Fig. 2B). The results indicated that although exosome

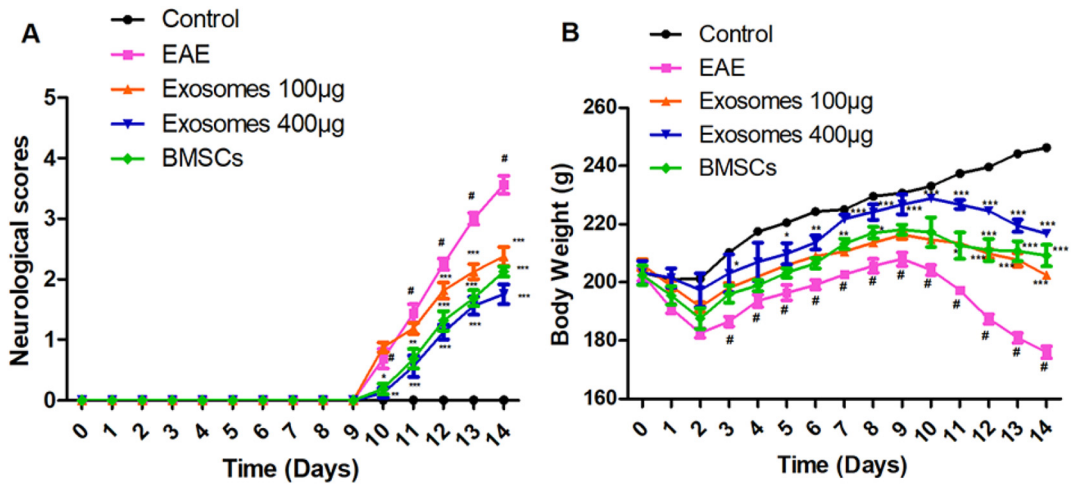

Fig. 2. BMSC exosomes ameliorate the loss of body weight and neurobehavioral symptoms in EAE rats. Exosome (low or high dose) and BMSC treatment did not delay EAE onset but did decrease the neurological severity of EAE. N = 8 per group, $^{\#}P < 0.05$, compared to the control group; $^{*}P < 0.05$, $^{**}P < 0.01$, $^{***}P < 0.001$ compared to the EAE group. Statistical analysis of different groups was performed with one-way analysis of variance (ANOVA) followed by Bonferroni's multiple group comparison.

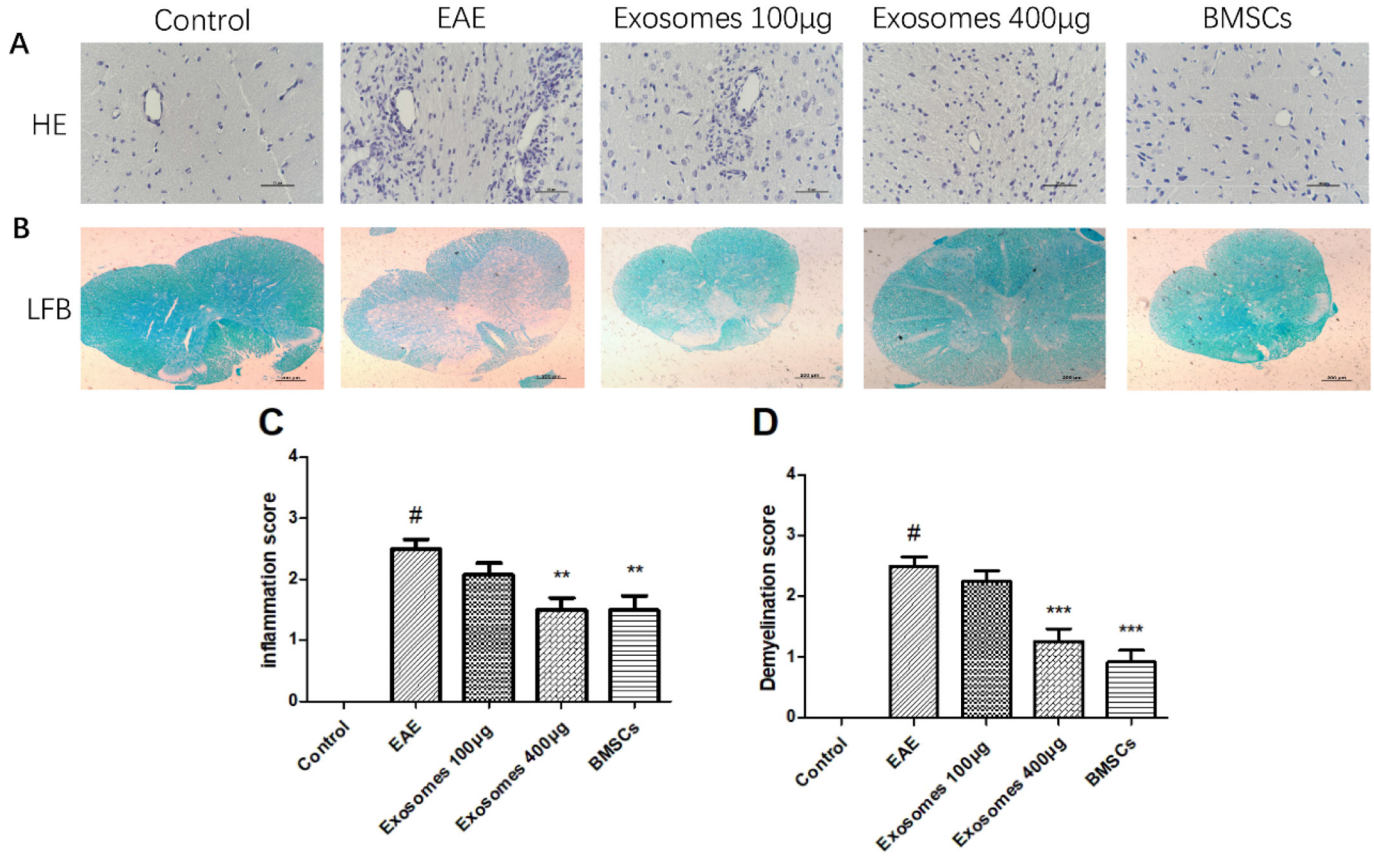

Fig. 3. BMSC exosomes ameliorate CNS inflammatory infiltration and demyelination. H&E (A) and LFB (B) staining showed that BMSC exosome treatment attenuated the infiltration of inflammatory cells and demyelination in spinal cords of EAE rats. Inflammation scores (C) and demyelination scores (D) were significantly lowered in both the exosome-treated and BMSC-treated groups. Magnification of H&E: ×400 (A), scale bars: 50 μm; magnification of LFB: ×40 (B), scale bars: 200 μm. Exosome-treated and BMSC-treated groups display less severe inflammatory infiltration and demyelination compared to the EAE group. Quantitative analysis (C&D). N = 4 per group, $^{\#}P < 0.05$, compared to the control group; $^{**}P < 0.01$, $^{***}P < 0.001$ compared to the EAE group.

treatment did not delay the onset of EAE, it did decrease the neurobehavioral scores and prevent weight loss. The effects of the exosome treatment were also dose-dependent ($P < 0.05$) (Fig. 2A, B).

3.4. Effect of BMSC exosomes on the histological changes of EAE

All the experimental rats were sacrificed on day 14, and the brain and lumbar enlargement of the spinal cord were collected for histological analysis. The results of H&E (Fig. 3A, C) and LFB (Fig. 3B, D) staining showed marked inflammatory cell infiltration and

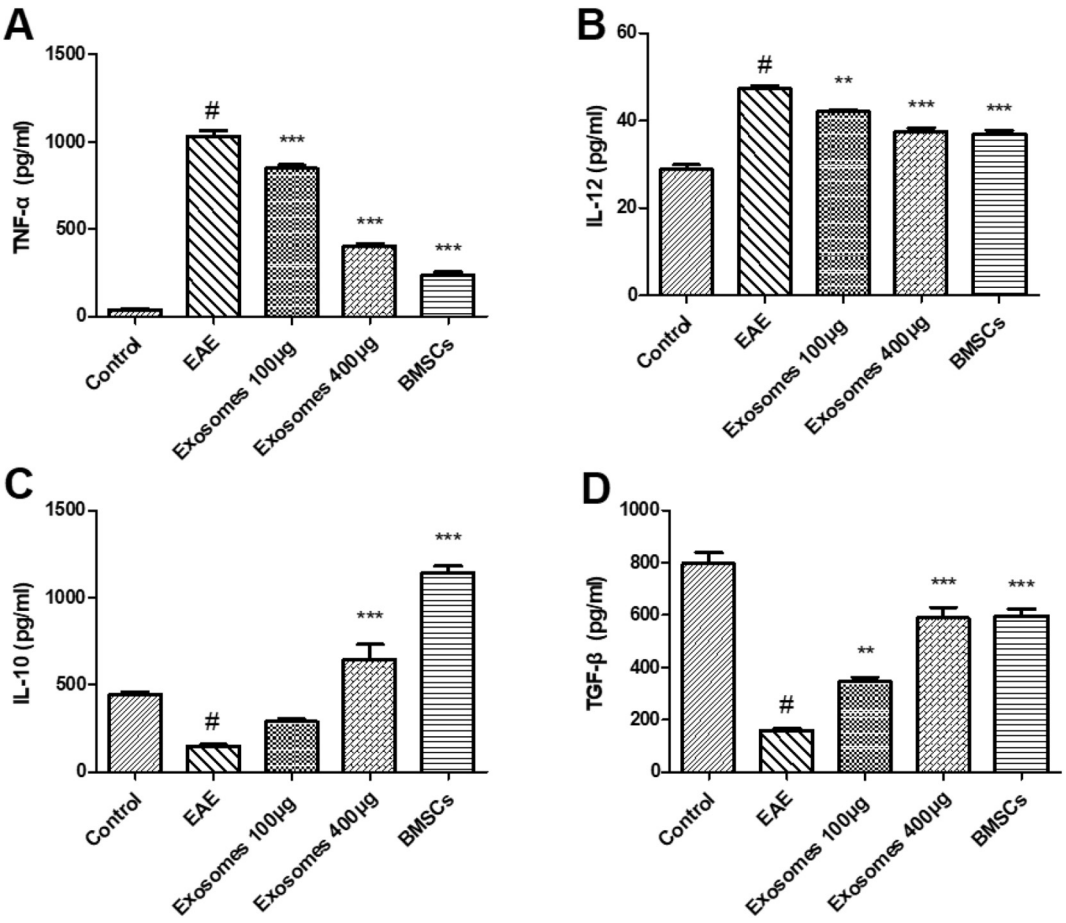

Fig. 4. Exosomes derived from BMSCs demonstrate immunoregulatory effects in vivo. N = 8 per group, columns represent means ± standard deviation. $^{\#}P < 0.05$, compared to the control group; $^{**}P < 0.01$, $^{***}P < 0.001$ compared to the EAE group.

demyelination in EAE rats. Lots of inflammatory cells as perivascular cuffs infiltrating around small blood vessels were observed by HE staining methods under light microscope in the brain tissue of EAE rats. After the injection of exosomes or BMSCs, the inflammatory cells around the blood vessels decreased to varying degrees. High dose exosome treatment significantly decreased the inflammatory cell infiltration and attenuated the demyelination ($P < 0.05$). The pathological scores of the high dose exosome group were lower than that of low dose group ($P < 0.05$) but did not reach significance when compared with the BMSC-treated group.

3.5. Effects of BMSC exosomes on cytokine production and microglia polarization in vivo

In EAE and MS, TNF-α and IL-12 contribute to inflammation and myelin damage, and IL-10 and TGF-β are involved in the relief of the disease. Therefore, we analyzed the levels of these cytokines in the serum of our experimental rats by ELISA. Significant increases in pro-inflammatory cytokines (TNF-α and IL-12), and significant decreases in anti-inflammatory cytokines (IL-10 and TGF-β) were observed in the EAE group compared to the control group ($P < 0.05$). As shown in Fig. 4A–D, exosome treatment significantly decreased the levels of TNF-α and IL-12 and increased the levels of IL-10 and TGF-β in the rat serum, which is consistent with alleviated inflammation.

The TNF-α levels detected were different among treatments. The IL-12 levels detected were different among treatments except exosomes 400 μg group versus BMSCs group.

The IL-10 levels detected were different among treatments except Control group versus exosomes 100 μg group and EAE group versus exosomes 100 μg group. The TGF-β levels detected were different among treatments except exosomes 400 μg group versus BMSCs group.

Quantitative real time PCR was used to detect mRNA expression of M1 and M2 phenotype-associated markers in the spinal cords of rats. The mRNA levels of the M1 markers TNF-α and iNOS were both significantly decreased after exosome (low dose or high dose) or BMSC treatment (Fig. 5A), while the mRNA levels of the M2 phenotypic markers IL-10, TGF-β, and Arg-1 were significantly increased compared to EAE rats (Fig. 5A). Although the alterations in mRNA expression were present in both exosome groups, a more conspicuous effect was seen in the high dose group compared to the low dose group ($P < 0.05$).

The expression levels of CD68 and CD206 were further evaluated to detect the M1/M2 phenotype by immunofluorescence staining of frozen spinal cord sections. Compared with the control group, the EAE group demonstrated an increased density of CD68+ cells and a decreased density of CD206+ cells (Fig. 5B). A significant reduction in CD68+ cells and increase in CD206+ cells was observed after exosome or BMSC treatment. These results suggest that exosome treatment significantly inhibited the development of microglia into the M1 phenotype and promoted polarization to the M2 phenotype in rat spinal cords, which was beneficial in dampening inflammation and promoting relief.

3.6. Effects of BMSC exosomes on cytokine production and microglia polarization in vitro

In order to further verify the mechanism through which BMSCs act on microglia, we co-cultured BMSCs with HAPI (rat microglia cell line)

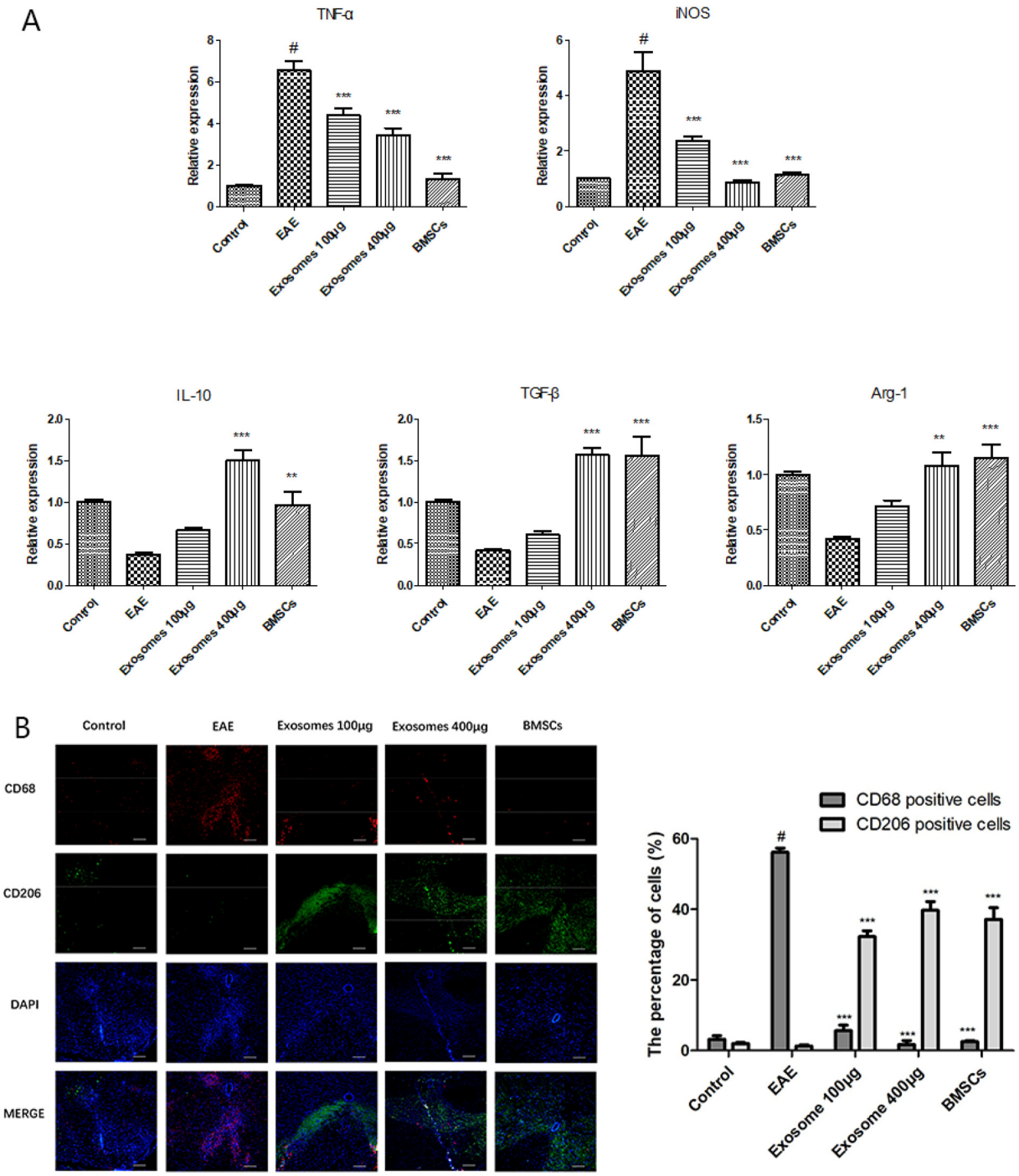

Fig. 5. Exosome treatment inhibits M1 phenotype polarization and promotes M2 polarization of microglia in rat spinal cords both in protein level and mRNA level. (A) Real-time quantitative PCR of microglia M1/M2 related markers in rat spinal cord tissue. N = 4 per group. Magnification: ×200, scale bar = 200 μm. (B) Immunofluorescent double staining of CD68 and CD206, and the quantificational analysis of the percentage of CD206 or CD68 positive area comparing to the entire section is presented as means ± standard deviation. N = 4 per group, $P < 0.05$, compared to the control group; **$P < 0.01$, ***$P < 0.001$ compared to the LPS group.

cells using a transwell system, which eliminates cell-to-cell contact (shown in Fig. 6A). Lipopolysaccharide (LPS) was added to these co-culture systems to simulate an inflammatory microenvironment in vitro, and phosphate buffer solution (PBS, vehicle solution) was added to the control group. The results showed that 24 h of LPS stimulation markedly increased the levels of pro-inflammatory cytokines (TNF-α and IL-12) and decreased those of the anti-inflammatory cytokines (IL-10 and TGF-β). And then treated with different concentrations of exosomes (62.5, 125, 250, 500, 1000 μg/mL) for 48 h. Exosomes and MSCs group inhibited the LPS-induced up-regulation of TNF-α and IL-12 (Fig. 6D, E), and promoted the up-regulation of IL-10 and TGF-β (Fig. 6B, C). Moreover, high dose exosome treatment (1000 μg/mL) had greater effects than low dose exosome treatment. Notably, the transwell co-culture experiment indicated that the mechanism through which the BMSCs affect microglia is through paracrine activity rather than through direct cell contact. Additionally, exosome treatment decreased the nitrite concentration present in the culture supernatant in a dose-dependent manner (Fig. 6F).

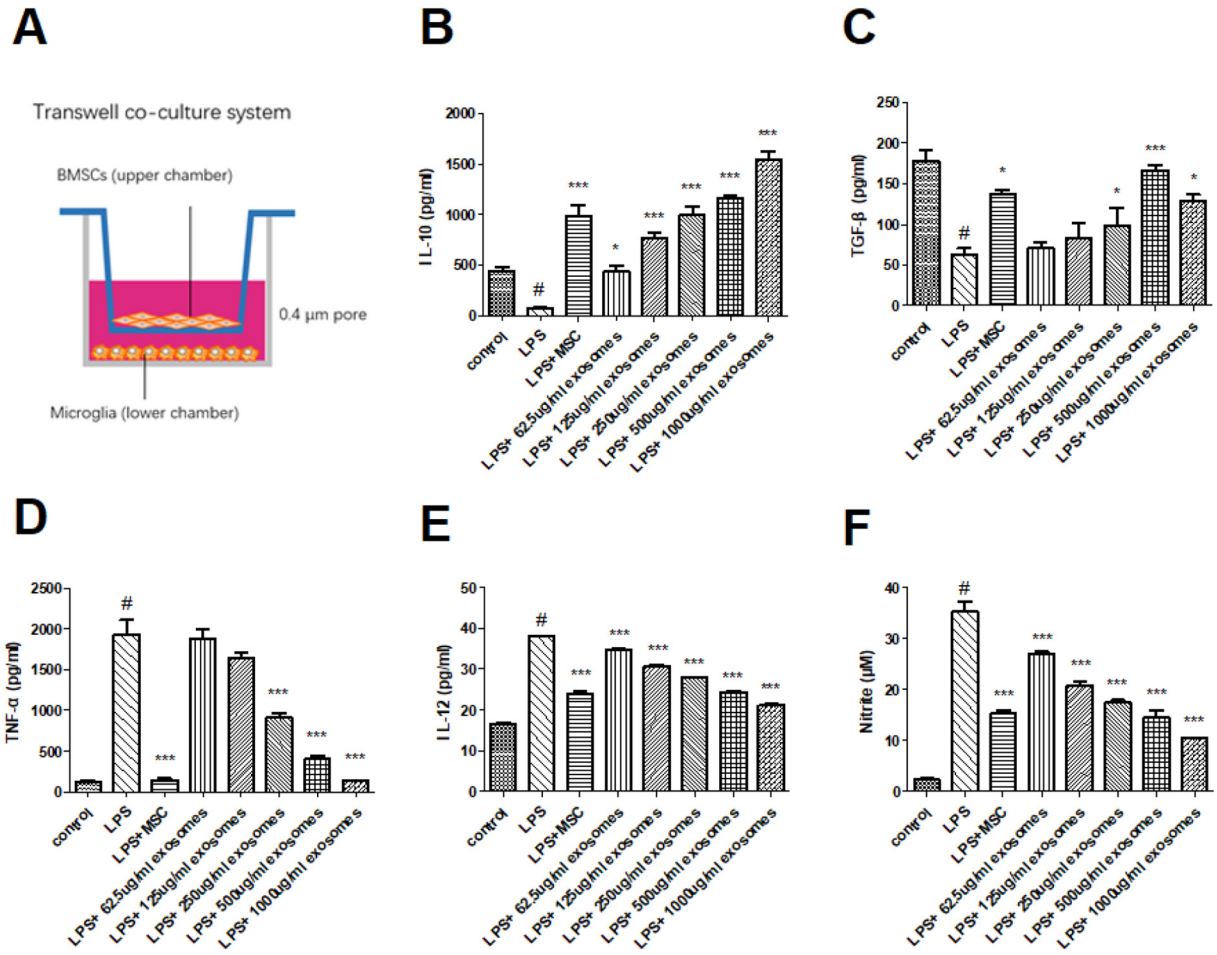

Fig. 6. Exosomes derived from BMSCs display immunoregulatory effects in vitro. N = 3 per group, $^{\#}P < 0.05$, compared to the control group; $^{**}P < 0.01$, $^{***}P < 0.001$ compared to the LPS group.

To further investigate the direct effects of exosomes on microglia, HAPI cells were stimulated with LPS for 24 h. Furthermore, the real time PCR results indicated that the mRNA levels of TNF-α and iNOS were significantly decreased in a dose-dependent manner in the exosome groups, compared with the LPS stimulated group (Fig. 7). However, the mRNA level of M2-associated markers IL-10, TGF-β, and Arg-1 also significantly decreased in a dose-dependent manner compared with the LPS group (Fig. 7).

3.7. Shotgun analysis

Proteomics analysis of the exosomes identified 676 proteins in the BMSC-exosomes. There were 22 kinds of immune response-related proteins (Table 2), 23 kinds of inflammatory response-related proteins (Table 3) and 4 kinds of myelination-related proteins (Table 4) among these proteins as listed in additional tables. They may mediate the polarization of microglia, relieve the inflammatory infiltration and demyelination, which were key factors for further mechanism research.

4. Discussion

MS is an autoimmune disease characterized by demyelination of the CNS and infiltration of inflammatory cells which reoccurs and progresses, often leading to lifelong disabilities. Over the past few decades, research on stem cell transplantation and regenerative medicine has yielded several positive results. Among stem cells, MSCs have been widely studied with respect to their differentiation potential, ability to self-replicate, hematopoietic support, and immune regulation. Therefore, it is widely hoped that stem cell therapy will be a viable treatment for MS. However, the availability of MSCs is limited, because their proliferation capacity decreases with each passage and limited numbers of cells can be obtained from a single donor [33]. Moreover, in recent years, studies have found that the stem cells exert their functions mainly via a paracrine mechanism rather than through migration to and directional differentiation at the injury site. Exosomes are small membraned vesicles secreted by many kinds of cells for the purpose of intercellular communication and may act as a kind of paracrine mediator. Recent studies have indicated that exosomes can exhibit functions similar to the cells from which they came. BMSCs are an ideal source of exosomes because they are well tolerated by the immune system, which is critical for successful clinical use [34]. It has been reported that MSCs can secrete immunologically active exosomes [35]. Cell-free therapy mediated by exosomes from BMSCs may be an alternative therapeutic strategy for treatment of MS. However, it remains unclear whether treatment with BMSC-derived exosomes could alleviate symptoms of MS or EAE. This study was designed to determine whether BMSC exosome treatment would benefit EAE rats and to find out whether exosome treatment would influence CNS inflammation or microglia polarization.

In the present study, primary BMSCs were successfully obtained, and their surface markers and differentiation abilities were confirmed. BMSC exosomes were then isolated from the cell culture supernatant and their therapeutic role in EAE rats was investigated. Previous studies in related fields have clearly demonstrated that transplanted BMSCs were capable of providing immunoregulatory and neuroprotective effects in both EAE and non-immune induced demyelination models

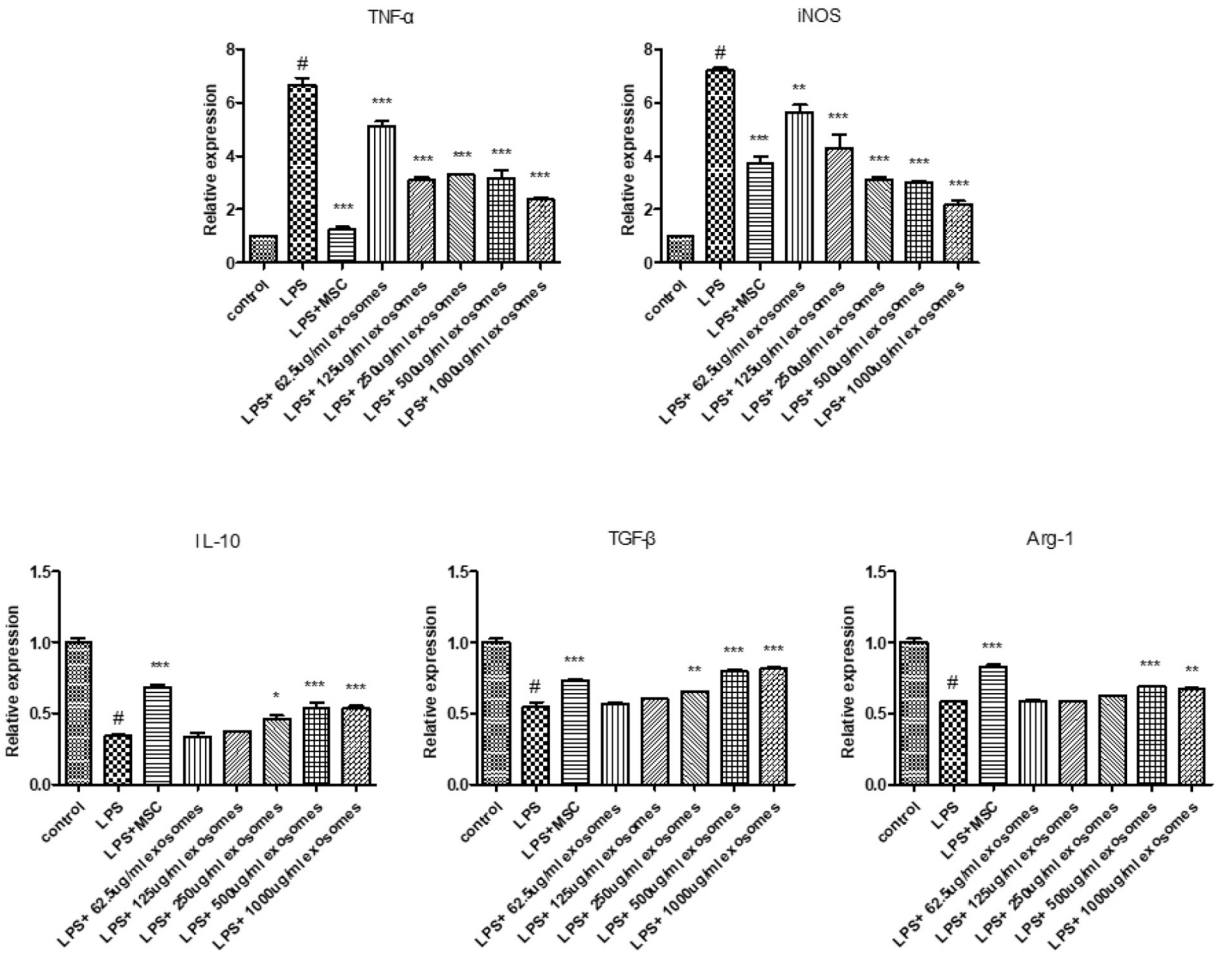

Fig. 7. Exosome treatment inhibits microglial M1 polarization, while M2 polarization is promoted at the mRNA level. N = 3 per group, $P < 0.05$, compared to the control group; *$P < 0.05$, **$P < 0.01$, ***$P < 0.001$ compared to the LPS group.

Table 2
Inflammatory response related protein in the MSC derived exosomes.

Protein ID	Protein name
A0A1B0GWS5	Complement C5
A0A0G2JTH4	Leukocyte surface antigen CD47
Q6GMN4	Macrophage colony-stimulating factor 1
D3ZP82	Lysyl oxidase-like 3
D3ZTJ3	ADAM metallopeptidase with thrombospondin type 1 motif, 12
F1LSX3	ADP-ribosyl cyclase/cyclic ADP-ribose hydrolase 2
G3V8U9	Proteasome subunit beta
M0R979	Thrombospondin 1
P07150	Annexin A1
P08050	Gap junction alpha-1 protein
P17246	Transforming growth factor beta-1
P18420	Proteasome subunit alpha type-1
P20961	Plasminogen activator inhibitor 1
P63039	60 kDa heat shock protein, mitochondrial
P85973	Inosine-guanosine phosphorylase
Q3MID7	Lipopolysaccharide-binding protein
Q5I035	Nuclear receptor subfamily 1, group H, member 3
Q5M7T5	Serine (Or cysteine) peptidase inhibitor, clade C (Antithrombin), member 1
Q62611	Interleukin-1 receptor-like 1
Q63691	Monocyte differentiation antigen CD14
Q71SA3	Thrombospondin 1
Q80ZA3	Alpha-2 antiplasmin
Q99J86	Attractin

Table 3
Immune response related protein in the MSC derived exosomes.

Protein ID	Protein name
Q5XI38	Lymphocyte cytosolic protein 1
Q6GMN4	Macrophage colony-stimulating factor 1
D3ZT94	Pentraxin 3
D3ZV30	DNA-directed RNA polymerase subunit beta
D4AE96	Importin 7
G3V7V4	Ectonucleotide pyrophosphatase/phosphodiesterase family member 1
G3V928	LDL receptor-related protein 1
M0R979	Throbospondin1
P04797	Glyceraldehyde-3-phosphate dehydrogenase
P07150	Annexin A1
P13941	Collagen alpha-1(III) chain
P17246	Transforming growth factor beta-1
P18420	Proteasome subunit alpha type-1
P31720	Complement C1q subcomponent subunit A
P33436	72 kDa type IV collagenase
P63039	60 kDa heat shock protein, mitochondrial
Q00238	Intercellular adhesion molecule 1
Q3MID7	Lipopolysaccharide-binding protein
Q4V8N0	Lipocalin 7, isoform CRA_a
Q62611	Interleukin-1 receptor-like 1
Q63691	Monocyte differentiation antigen CD14
Q71SA3	Thrombospondin 1

Table 4
Myelination related protein in the MSC derived exosomes.

Protein ID	Protein name
P17246	Transforming growth factor beta-1
Q641X3	Beta-hexosaminidase subunit alpha
Q99J82	Integrin-linked protein kinase
Q99J86	Attractin

[36–38]. In this study, we performed experiments in vivo and in vitro to investigate whether BMSC exosomes were protective against EAE. We first injected BMSCs and BMSC exosomes into the tail veins of EAE rats and found that both significantly ameliorated weight loss and decreased neurobehavioral symptoms compared to EAE rats not given BMSCs or exosomes. Additionally, they both significantly attenuated inflammation and demyelination in the CNS. Microglia, important immune cells in the CNS, were activated into a classical M1 phenotype and secreted pro-inflammatory cytokines. After BMSC exosome treatment, the concentrations of the cytokines TNF-α, IL-10, and TGF-β were measured. BMSC exosome treatment significantly reduced the secretion of TNF-α and enhanced the secretion of IL-10 and TGF-β. Opposite of M1, the M2 "alternatively activated" phenotype is associated with the secretion of anti-inflammatory cytokines such as IL-10 and TGF-β. The results of our in vivo experiments indicate that BMSC exosome treatment polarizes microglia from a M1 phenotype toward a M2 phenotype, which may account for the protective effects of BMSC exosomes in EAE. To clarify the effect of BMSC exosomes on microglia, we detected surface markers associated with M1 and M2 microglia in brain and spinal cord of the rats. We observed that after stem cell treatment and exosome treatment, expression of the M1 marker CD68 decreased while the M2 phenotype marker CD206 increased compared to the EAE group. Furthermore, the mRNA levels of microglia M1 phenotype markers (iNOS and TNF-α) and M2 phenotype markers (Arg-1, IL-10 and TGF-β) were detected. These results were consistent with those of the protein expression data.

In our present in vitro study, the rat microglia cell line HAPI was used to verify the role of BMSC exosomes on microglial polarization. Firstly, BMSCs and microglia were seeded in the upper chamber and lower chamber of a transwell co-culture system, respectively, for 48 h. Compared with LPS-activated microglia, the concentration of the pro-inflammatory cytokine TNF-α decreased and the anti-inflammatory cytokines IL-10 and TGF-β increased in the co-culture system. Similarly, our in vitro experimental results demonstrated that BMSC exosome treatment induced microglia polarization toward the M2 phenotype, as evidenced at both the mRNA and protein levels. In summary, our results revealed that BMSC-derived exosomes modulate microglia polarization in both EAE models and in a cell line. Upon EAE onset, microglia become overactivated and polarized to the M1 phenotype. M1 microglia aggravate neurological damage by releasing multiple pro-inflammatory factors and recruiting inflammatory cells to the CNS. After BMSC exosome treatment, microglia were polarized toward the anti-inflammatory M2 phenotype. The cytokines released by the M2 microglia provide an immune-tolerant microenvironment which suppresses neuroinflammation and promotes oligodendrocyte differentiation during CNS remyelination [39]. Furthermore, our results indicate that BMSC exosomes promote relief from EAE.

A similar study performed by Mokarizadeh and colleagues showed that MSC-derived exosomes could insert bioactive tolerogenic molecules onto auto-reactive lymphocytes and modulate their phenotypes. The results confirmed the potent ability of MSC-derived MVs to induce regulatory T cells [40]. In addition, microvesicles derived from MSCs could inhibit auto-reactive lymphocyte proliferation and promote secretion of IL-10 and TGF-β. Another study [41] indicated that exosome pre-treated lymphocytes secreted < 50% of IFN-γ and IL-17, which were described as the hallmarks of Th1 and Th17 phenotypes respectively, compared to the untreated lymphocytes.

This study is the first application of BMSC exosomes in the EAE model and provides evidence of their effect on microglia phenotype switching for the first time. The results of this study indicate a potential

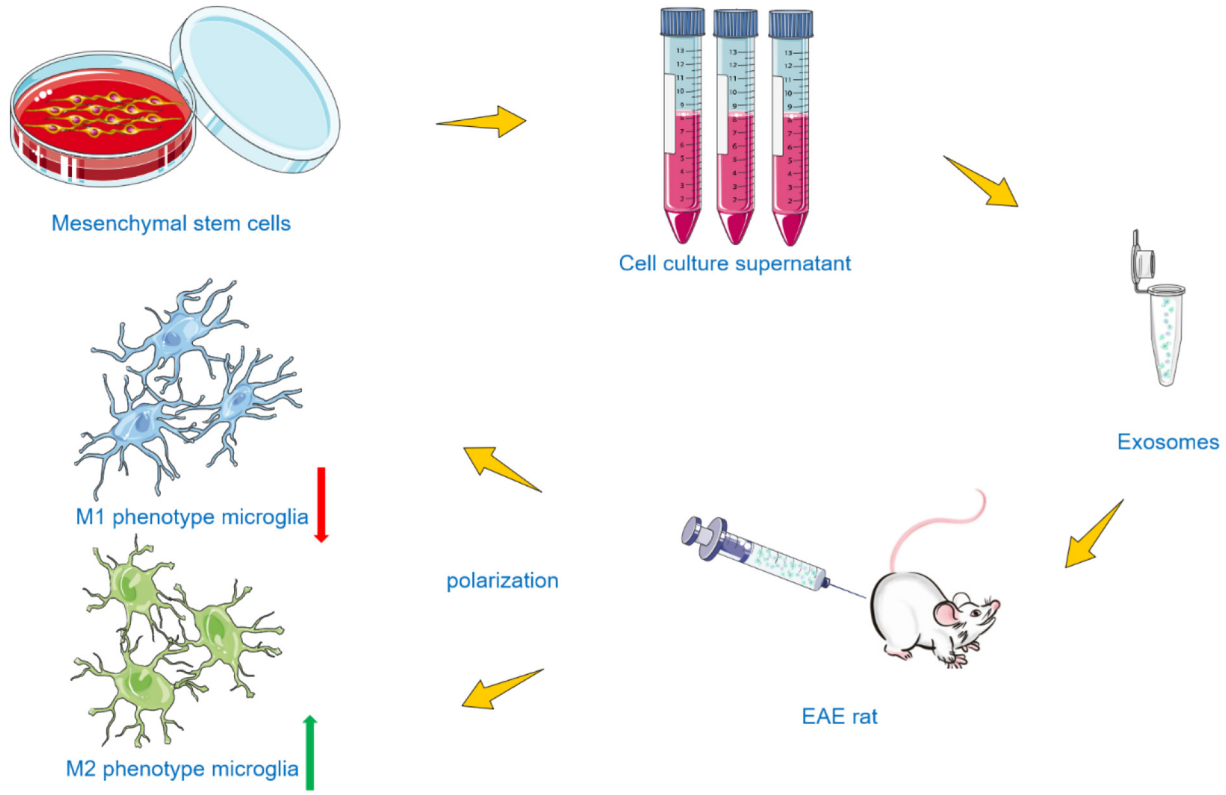

Fig. 8. Exosomes derived from mesenchymal stem cells attenuate inflammation and demyelination in EAE rats by regulating the polarization of microglia.

treatment to benefit those with autoimmune diseases. In addition to the mechanisms described here, BMSC exosomes may also improve neurological function by promoting tissue repair. Further studies are needed to reveal the specific functional proteins and other molecules transported by BMSC exosomes that play crucial roles in microglia polarization, alleviation of inflammation, and tissue repair. Revealing these key molecules may expand our knowledge on the pathophysiology and treatment of MS and EAE (Fig. 8).

In this study, we mainly concentrated on the property of exosomes in the immunoregulatory field. In addition, we have summarized the application of MSCs-derived exosomes in the ischemic diseases in our recent published review [42]. Apart from the applications in immunemodulatory and regenerative therapies, exosomes derived from different cell types may serve as novel tools for various therapeutic approaches, including anti-tumor therapy, pathogen vaccination and drug delivery. However, the clinical translation of exosomes into therapy application is still a long way to go. As a kind of biological medicine, exosomes production standard and quality control remain a challenge for their safely used to clinical patients. Besides, exosomes improved isolation and storage methods and reliable clinic trials results will be great help to the clinical translation of exosome-based therapeutics [28,43].

5. Conclusions

In summary, this study confirmed that BMSC-derived exosomes improve rat motor function relief and reduce demyelination and neuroinflammation in an immune-induced demyelination model. The mechanism by which BMSC-derived exosomes ameliorate EAE is through modulation of microglial polarization between the M1 and M2 phenotypes. Moreover, our findings indicate that BMSC-derived exosomes may be developed into a promising cell-free therapy for MS.

Acknowledgment

This work was supported financially by the National Natural Science Foundation of China (grant number 81771271), Program of Basic and Clinical Research Platform of China Medical University (CMU-201406)—the Second Batch of Basic Clinical Closely Combined Platform Project, and study on the epigenetic molecular mechanism of tanshinone IIA for treatment of EAE blood-brain barrier destruction and immune inflammatory response funded by the Science and Technology Department of Liaoning Province to Juan Feng; Excellent PhD Program of Shengjing Hospital of China Medical University (No. MF14).

Conflict of interest

The authors have no conflicts of interest to declare.

References

[1] H. Lassmann, Multiple sclerosis pathology: evolution of pathogenetic concepts, Brain Pathol. 15 (2005) 217–222.
[2] L. Steinman, Immunology of relapse and remission in multiple sclerosis, Annu. Rev. Immunol. 32 (2014) 257–281.
[3] I. Bjelobaba, V. Begovic-Kupresanin, S. Pekovic, I. Lavrnja, Animal models of multiple sclerosis: focus on experimental autoimmune encephalomyelitis, J. Neurosci. Sci. 96 (2018) 1021–1042.
[4] X.Y. Xiong, L. Liu, Q.W. Yang, Functions and mechanisms of microglia/macrophages in neuroinflammation and neurogenesis after stroke, Prog. Neurobiol. 142 (2016) 23–44.
[5] C. Baecher-Allan, B.J. Kaskow, H.L. Weiner, Multiple sclerosis: mechanisms and immunotherapy, Neuron 97 (2018) 742–768.
[6] R. Orihuela, C.A. McPherson, G.J. Harry, Microglial M1/M2 polarization and metabolic states, Br. J. Pharmacol. 173 (2016) 649–665.
[7] F. Chu, M. Shi, C. Zheng, D. Shen, J. Zhu, X. Zheng, et al., The roles of macrophages and microglia in multiple sclerosis and experimental autoimmune encephalomyelitis, J. Neuroimmunol. 318 (2018) 1–7.
[8] C. Xu, F. Fu, X. Li, S. Zhang, Mesenchymal stem cells maintain the microenvironment of central nervous system by regulating the polarization of macrophages/microglia after traumatic brain injury, Int. J. Neurosci. 127 (2017) 1124–1135.
[9] L. Sensebe, M. Krampera, H. Schrezenmeier, P. Bourin, R. Giordano, Mesenchymal stem cells for clinical application, Vox Sang. 98 (2010) 93–107.
[10] A. Fierabracci, A. Del Fattore, M. Muraca, The immunoregulatory activity of mesenchymal stem cells: 'state of art' and 'future avenues', Curr. Med. Chem. 23 (2016) 3014–3024.
[11] M. Simons, G. Raposo, Exosomes—vesicular carriers for intercellular communication, Curr. Opin. Cell Biol. 21 (2009) 575–581.
[12] A.V. Vlassov, S. Magdaleno, R. Setterquist, R. Conrad, Exosomes: current knowledge of their composition, biological functions, and diagnostic and therapeutic potentials, Biochim. Biophys. Acta 1820 (2012) 940–948.
[13] C.Y. Chen, S.S. Rao, L. Ren, X.K. Hu, Y.J. Tan, Y. Hu, et al., Exosomal DMBT1 from human urine-derived stem cells facilitates diabetic wound repair by promoting angiogenesis, Theranostics 8 (2018) 1607–1623.
[14] J. Mayourian, D.K. Ceholski, P. Mathiyalagan, J.F. Murphy, S.I. Salazar, et al., Exosomal microRNA-21-5p mediates mesenchymal stem cell paracrine effects on human cardiac tissue contractility, Circ. Res. 122 (2018) 933–944.
[15] K.I. Mentkowski, J.D. Snitzer, S. Rusnak, J.K. Lang, Therapeutic potential of engineered extracellular vesicles, AAPS J. 20 (2018) 50.
[16] F. Beretti, M. Zavatti, F. Casciaro, G. Comitini, F. Franchi, V. Barbieti, et al., Amniotic fluid stem cell exosomes: therapeutic perspective, Biofactors 44 (2018) 158–167.
[17] R. Tamura, S. Uemoto, Y. Tabata, Immunosuppressive effect of mesenchymal stem cell-derived exosomes on a concanavalin A-induced liver injury model, Inflamm. Regen. 36 (2016) 26.
[18] D. Wen, Y. Peng, D. Liu, Y. Weizmann, R.I. Mahato, Mesenchymal stem cell and derived exosome as small RNA carrier and Immunomodulator to improve islet transplantation, J. Control. Release 238 (2016) 166–175.
[19] P. Zhao, L. Xiao, J. Peng, Y.Q. Qian, C.C. Huang, Exosomes derived from bone marrow mesenchymal stem cells improve osteoporosis through promoting osteoblast proliferation via MAPK pathway, Eur. Rev. Med. Pharmacol. Sci. 22 (2018) 3962–3970.
[20] Y. Xiao, F. Geng, G. Wang, X. Li, J. Zhu, W. Zhu, Bone marrow-derived mesenchyal stem cells-derived exosomes prevent oligodendrocyte apoptosis through exosomal miR-134 by targeting caspase-8, J. Cell. Biochem. (2018), https://doi.org/10.1002/jcb.27519.
[21] X. Ouyang, X. Han, Z. Chen, J. Fang, X. Huang, H. Wei, MSC-derived exosomes ameliorate erectile dysfunction by alleviation of corpus cavernosum smooth muscle apoptosis in a rat model of cavernous nerve injury, Stem Cell Res Ther 9 (2018) 246.
[22] Y. Wang, R. Zhao, D. Liu, W. Deng, G. Xu, W. Liu, et al., Exosomes derived from miR-214-enriched bone marrow-derived mesenchymal stem cells regulate oxidative damage in cardiac stem cells by targeting CaMKII, Oxidative Med. Cell. Longev. 2018 (2018) 4971261.
[23] K. Kubota, M. Nakano, E. Kobayashi, Y. Mizue, T. Chikenji, M. Otani, et al., An enriched environment prevents diabetes-induced cognitive impairment in rats by enhancing exosomal miR-146a secretion from endogenous bone marrow-derived mesenchymal stem cells, PLoS One 13 (2018) e0204252.
[24] S. Gao, Z. Zhao, R. Wu, Y. Zeng, Z. Zhang, J. Miao, et al., Bone marrow mesenchymal stem cell transplantation improves radiation-induced heart injury through DNA damage repair in rat model, Radiat. Environ. Biophys. 56 (2017) 63–77.
[25] C. Thery, S. Amigorena, G. Raposo, A. Clayton, Isolation and characterization of exosomes from cell culture supernatants and biological fluids, Curr. Protoc. Cell Biol. (2006) 22 (Chapter 3: Unit 3).
[26] H. Yang, C. Liu, J. Jiang, Y. Wang, X. Zhang, Celastrol attenuates multiple sclerosis and optic neuritis in an experimental autoimmune encephalomyelitis model, Front. Pharmacol. 8 (2017) 44.
[27] Y. Li, Y.Y. Yang, J.L. Ren, F. Xu, F.M. Chen, A. Li, Exosomes secreted by stem cells from human exfoliated deciduous teeth contribute to functional recovery after traumatic brain injury by shifting microglia M1/M2 polarization in rats, Stem Cell Res Ther 8 (2017) 198.
[28] A.T. Reiner, K.W. Witwer, B.W.M. van Balkom, J. de Beer, C. Brodie, R.L. Corteling, et al., Concise review: developing best-practice models for the therapeutic use of extracellular vesicles, Stem Cells Transl. Med. 6 (2017) 1730–1739.
[29] X. Yang, J. Yan, J. Feng, Treatment with tanshinone IIA suppresses disruption of the blood-brain barrier and reduces expression of adhesion molecules and chemokines in experimental autoimmune encephalomyelitis, Eur. J. Pharmacol. 771 (2016) 18–28.
[30] V.G. Jokubaitis, M.M. Gresle, D.A. Kemper, W. Doherty, V.M. Perreau, T.L. Cipriani, et al., Endogenously regulated Dab2 worsens inflammatory injury in experimental autoimmune encephalomyelitis, Acta Neuropathol. Commun. 1 (2013) 32.
[31] X. He, W. Yuan, Z. Li, Y. Hou, F. Liu, J. Feng, 6-Hydroxydopamine induces autophagic flux dysfunction by impairing transcription factor EB activation and lysosomal function in dopaminergic neurons and SH-SY5Y cells, Toxicol. Lett. 283 (2018) 58–68.
[32] M. Dominici, K. Le Blanc, I. Mueller, I. Slaper-Cortenbach, F. Marini, D. Krause, et al., Minimal criteria for defining multipotent mesenchymal stromal cells. The International Society for Cellular Therapy position statement, Cytotherapy 8 (2006) 315–317.
[33] M. Zaim, S. Karaman, G. Cetin, S. Isik, Donor age and long-term culture affect differentiation and proliferation of human bone marrow mesenchymal stem cells, Ann. Hematol. 91 (2012) 1175–1186.
[34] R.C. Lai, R.W. Yeo, K.H. Tan, S.K. Lim, Exosomes for drug delivery - a novel application for the mesenchymal stem cell, Biotechnol. Adv. 31 (2013) 543–551.
[35] B. Zhang, Y. Yin, R.C. Lai, S.S. Tan, A.B. Choo, S.K. Lim, Mesenchymal stem cells secrete immunologically active exosomes, Stem Cells Dev. 23 (2014) 1233–1244.

[36] J. Nessler, K. Benardais, V. Gudi, A. Hoffmann, L. Salinas Tejedor, S. Janssen, et al., Effects of murine and human bone marrow-derived mesenchymal stem cells on cuprizone induced demyelination, PLoS One 8 (2013) e69795.
[37] A.C. Bowles, B.A. Scruggs, B.A. Bunnell, Mesenchymal stem cell-based therapy in a mouse model of experimental autoimmune encephalomyelitis (EAE), Methods Mol. Biol. (Clifton, NJ) 1213 (2014) 303–319.
[38] G. El-Akabawy, L.A. Rashed, Beneficial effects of bone marrow-derived mesenchymal stem cell transplantation in a non-immune model of demyelination, Ann. Anat. 198 (2015) 11–20.
[39] V.E. Miron, A. Boyd, J.W. Zhao, T.J. Yuen, J.M. Ruckh, J.L. Shadrach, et al., M2 microglia and macrophages drive oligodendrocyte differentiation during CNS remyelination, Nat. Neurosci. 16 (2013) 1211–1218.
[40] A. Mokarizadeh, N. Delirezh, A. Morshedi, G. Mosayebi, A.A. Farshid, B. Dalir-Naghadeh, Phenotypic modulation of auto-reactive cells by insertion of tolerogenic molecules via MSC-derived exosomes, Vet. Res. Forum 3 (2012) 257–261.
[41] A. Mokarizadeh, N. Delirezh, A. Morshedi, G. Mosayebi, A.A. Farshid, K. Mardani, Microvesicles derived from mesenchymal stem cells: potent organelles for induction of tolerogenic signaling, Immunol. Lett. 147 (2012) 47–54.
[42] W. Wang, Z. Li, J. Feng, The potential role of exosomes in the diagnosis and therapy of ischemic diseases, Cytotherapy 20 (2018) 1204–1219.
[43] T. Lener, M. Gimona, L. Aigner, V. Borger, E. Buzas, G. Camussi, et al., Applying extracellular vesicles based therapeutics in clinical trials - an ISEV position paper, J. Extracellular Vesicles 4 (2015) 30087.